17th World Conference on Earthquake Engineering, 17WCEE
Sendai, Japan - September 13th to 18th 2020

FRAGILITY AND LOSS ASSESSMENT VIA MIXED PROBABILISTIC MODELS OF SEISMIC DEMAND

D. Vamvatsikos [(1)], A. Chatzidaki [(2)]

[(1)] *Assistant Professor, National Technical University of Athens, divamva@central.ntua.gr*
[(2)] *PhD candidate, National Technical University of Athens, cakrivi@central.ntua.gr*

Abstract

A mixture model is presented for combining the results of different models or analysis approaches into a single probabilistic seismic demand model that is suitable for fragility assessment. A structure can be represented using different model types or even levels of resolution for the same type, while it may also be analyzed via methods of different complexity, most notably static versus dynamic nonlinear approaches. Combining the results from different sources can be beneficial as it allows updating the results of a simpler approach or combining the strengths of two different models. For example, as the static pushover analysis offers inexpensive yet low-fidelity demand assessment at any level of intensity, its results may be locally or globally updated by adding stripes of (computationally expensive) response history analysis. On the modelling side, different model types may offer accuracy advantages in complementary response regions. This is the case of distributed-plasticity fiber models that offer higher fidelity for reinforced concrete frames at low (pre-capping) deformations, while lumped-plasticity models are more reliable for larger (post-capping) deformations closer to collapse. Through the combination of the results of multiple models of differing fidelity we can potentially better capture the performance of a structure at all levels of seismic intensity. By employing a minimal 5 parameter power-law-based model we offer viable options for forming mixed probabilistic seismic demand models that can combine both different models and different analysis methods into a single output suitable for fragility and loss assessment.

Keywords: fragility; static pushover; nonlinear dynamic analysis; regression

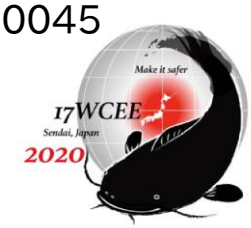

1. Introduction

The Performance-Based Earthquake Engineering (PBEE) framework, originally developed by Cornell and Krawinkler [1] for the Pacific Earthquake Engineering Research Center, is commonly employed for seismic risk assessment. The PBEE methodology can be summarized as an implementation of the total probability theorem as per Eq. (1):

$$\lambda(DV) = \iiint \mathrm{G}(DV \mid DM)\left|\mathrm{dG}(DM \mid EDP)\right|\left|\mathrm{dG}(EDP \mid IM)\right|\left|\mathrm{d}\,\lambda(IM)\right| \quad (1)$$

where *IM* is the ground motion Intensity Measure, *EDP* is the Engineering Demand Parameter (e.g. maximum interstory drift ratio), *DM* is the damage measure, *DV* is the Decision Variable, $\mathrm{G}(var_1|var_2)$ is the probability that specified values of var_1 are exceeded given the level of var_2 and $\lambda(DV)$ is the mean annual frequency of exceeding the *DV*. Consequently, risk can be estimated in terms of decision variables that make sense even to non-engineers such as casualties, monetary loss, repair cost, down time etc.

Of significant importance when employing the PBEE framework, is to accurately determine the building/class-specific fragility and vulnerability functions. Vulnerability functions are loss-valued functions of the IM that define the distribution of losses while fragility functions are probability-valued functions of the IM providing the probability of exceeding/violating a Limit State (LS). They are typically assessed via analytical methods that rely on numerical models subject to static or dynamic procedures [2]. In the latter case, the structural model is subjected to a number of time-history analysis under a suite of ground motion records, that would ideally come from an appropriate selection approach so as to be consistent with the site-specific seismic hazard (e.g. [3, 4, 5]). This analysis option is not widely implemented by practitioners due to its substantial computational cost as multiple dynamic analyses are required to capture the response EDP distribution over a range of IM values of intensity.

On the contrary, the static pushover analysis (SPO) is often the go-to single-run method, which through the approximation of the multi-degree-of-freedom (MDOF) structure via an equivalent single-degree-of-freedom (ESDOF) can offer computational simplicity at the cost of non-negligible errors [6, 7]. Although the SPO approach is mainly known in the context of seismic codes (e.g., ASCE 41-13 [8] or EN1998-3 [9]) for providing a single estimate of EDP response given the level of intensity, it is often disregarded that through the ESDOF approximation it can be used as a basis for assessing the full distribution of the dynamic response. Similarly to a code-like application, this procedure involves performing SPO analysis on the MDOF system, obtaining the corresponding pushover curve of the ESDOF system, fitting a piecewise linear function to the ESDOF SPO capacity curve (e.g. bilinear, trilinear or more advanced fits [10]), obtaining the probabilistic characterization of seismic demand from the ESDOF system and finally translating it to the MDOF response.

When it comes to estimating the seismic demand, a lognormal distribution model is adopted for the response of the (MDOF or ESDOF) system conditioned on its intensity. Thus, estimating the conditional mean and variance is adequate for a comprehensive characterization. The variance in the response can be approximated through the ESDOF model either via direct nonlinear dynamic analyses or through modern R-μ-T (strength ratio–ductility–period) relationships that provide not only the mean but also the variance. Examples of the former are proposed by Ruiz-García and Miranda [11] for elastoplastic backbones, and by Vamvatsikos and Cornell [12] for complex quadrilinear ones. For more casual users, Baltzopoulos et al. [13] have developed an open-source graphical user interface for performing nonlinear dynamic analyses of single-degree-of-freedom oscillators that can be used for assessing the dynamic response of ESDOFs.

The SPO approach to estimating the distribution of EDP response naturally brings in all the weaknesses of the ESDOF approximation in estimating both the mean and the variance. Specifically, the ESDOF is not capable of capturing the additional response variability due to the contribution of the higher modes. When it comes to the mean, the SPO approach may introduce considerable bias in the assessment,

especially for plan-asymmetric or tall buildings, due to the inherent inadequacy of an ESDOF description of the complex dynamic response.

These issues reduce the fidelity of SPO-based results and render one unable to recommend the SPO approach with some confidence as a generally viable method. The question, thus, remains: Can one trust the trusty old workhorse of seismic assessment to deliver credible results in a PBEE world? Perhaps yes, with a pair of new horseshoes. Baltzopoulos et al. [14] have offered a way to remedy the missing variability by employing precomputed results from MDOF dynamic analyses to correct the lower ESDOF variability, at least in the elastic range. Similarly, one may employ a limited number of MDOF dynamic analyses for refining the mean estimate of the response obtained through the ESDOF. In effect, by integrating the results from two different analysis approaches one can take advantage of the easy full-range computational capability of the ESDOF and bias-correct it with a limited sample of MDOF dynamic analyses to achieve a result that is more than the sum of its parts. In the following, we shall outline our proposal for a minimalistic framework to combine the static pushover and nonlinear dynamic analysis results in a single mixed probabilistic model of seismic demand, to be illustrated by means of applying it to a 4-story reinforced concrete building.

2. Case-study building

The building has two perimeter moment resisting frames (MRFs) of four bays each, which act in each principal direction, and internal columns that carry only the gravity loads. The plan view of the building and the elevation of the moment frames are shown in Fig. 1. The overall plan dimensions are about 55x37m (120'x180') and the total height of the building is about 16.5m (54'), with a 4.5m (15') first story and 4m (13') height in the remaining stories. Dead loads of 8.4kN/m^2 (175psf) and live loads of 2.4kN/m^2 (50psf) were assumed during the design, with the latter not acting on the roof. The building was designed by Aschheim et al. [15] following a performance-based design approach via the use of the Yield Frequency Spectra [16]. This allows designing structures that comply with performance objectives that are defined a priori by the analyst.

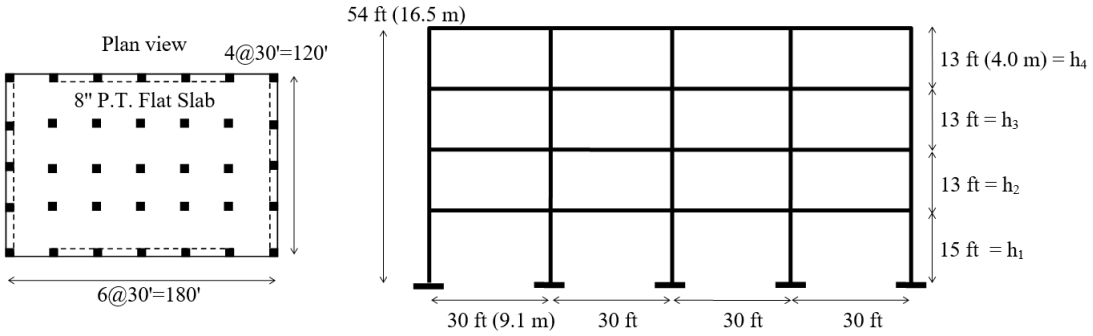

Fig. 1 – Plan view of the 4-story reinforced concrete building and elevation of the perimeter moment resisting frame (adopted from Aschheim et al. [15])

3. MDOF modeling and ESDOF

The two-dimensional (2D) MDOF model of the building was developed on the OpenSees platform [17]. Only one out of the two perimeter MRFs that act in each principal direction was modeled along with a leaning column to account for the effects of the columns not belonging to the MRF. The leaning column was pinned at the foundation and modeled using linear elastic elements having cross sectional properties of one half of the gravity columns of the building plus one half of the columns that belong to the MRFs acting in the other direction. Lumped-plasticity elements were employed for modeling the beams and columns of the

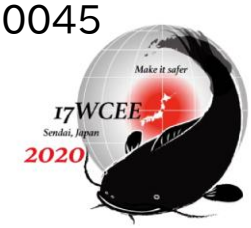

MRF, since they are computationally robust in the negative stiffness region of response, and can thus better capture collapse. The beams and columns were modeled using a single force-based beam-column element per member with plastic hinges located at each end, with their moment-rotation relationship defined according to ASCE 41-13 [8]. Rigid diaphragm constrains were imposed on each floor.

The SPO curve of the MDOF system resulting from a first-mode proportional lateral load pattern is presented in Fig. 2a in terms of base shear, V_{base}, and roof displacement, δ_{roof}. This was used as a basis for determining the backbone of the ESDOF system, whose reaction force, F^*, and displacement, δ^*, were computed by dividing the corresponding MDOF values by the modal participation factor, Γ, given by Fajfar [18] as per Eq. (2):

$$\Gamma = \frac{\sum_{i=1}^{N} m_i \varphi_i}{\sum_{i=1}^{N} m_i \varphi_i^2} \tag{2}$$

where N is the number of stories, m_i the mass of floor i and φ_i the corresponding ordinate of the first eigenmode, after the latter is normalized to 1.0 at the roof level ($\varphi_n = 1$). The SPO capacity curve of the ESDOF model is presented in Fig. 2b. The mass of the ESDOF and the period of vibration were estimated as $m^* = \sum_{i=1}^{N} m_i \varphi_i$ and $T^* = 2\pi\sqrt{m^* \cdot \delta_y^* / F_y^*}$, respectively. The yield force, F_y^*, and yield displacement, δ_y^*, depend on the piecewise linear approximation adopted for fitting the SPO capacity curve. In our case, an elastic-plastic backbone was fitted to the ESDOF capacity curve, as shown in Fig. 2b. Following the recommendations of De Luca et al. [10], the elastic segment of the bilinear fit was matched to the elastic stiffness of the capacity curve, rather than adopting a lower secant stiffness, since the response of the structure is not characterized by significant stiffness changes. This is an inherent property of the lumped-plasticity model, which cannot reproduce well enough concrete cracking and gradual plastification of sections. The post-yield linear segment of zero stiffness matches the maximum base shear recorded in the SPO. The horizontal plateau ends at the deformation where 20% of the maximum base shear is lost.

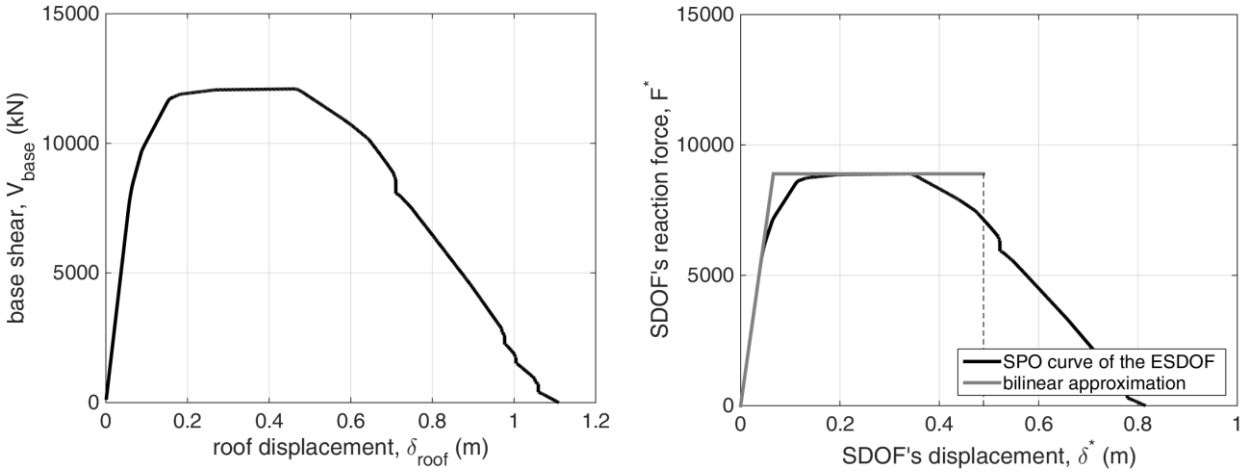

(a) MDOF's SPO capacity curve (b) ESDOF's SPO capacity curve and its bilinear fit

Fig. 2 – a) Static pushover capacity curve resulting from a first-mode proportional lateral load pattern on the MDOF model and (b) SPO curve of the ESDOF model and its bilinear fit

The bilinear-backbone ESDOF was subjected to Incremental Dynamic Analysis (IDA, [19]) for assessing its seismic performance, via the opensource software of Vamvatsikos [20]. When employing IDA, the model of the structure is subjected to a series of nonlinear dynamic analyses under a suite of ground motion records that are progressively scaled aiming to capture the entire range of the structural response,

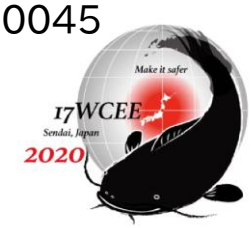

from elasticity up to global dynamic instability. The analysis results are typically presented in the form of IDA curves, one for each record, in terms of the IM versus EDP. The individual IDA curves can be summarized into the 16, 50 and 84% IDA fractiles of EDP | IM, or equivalently into the 84, 50 and 16% fractiles of IM | EDP [21]. If lognormality is assumed, the IDA fractiles can be used directly for estimating the median (as the 50% fractile) and the dispersion of the response, as the ½ of the difference among the 16% and 84% fractiles. The far-field set of ground motion records of FEMA P695 [22] was used for the analyses. This comprises 22 ground motions, each having two horizontal components thus resulting in a total of 44 accelerograms. In case T^* differs from T_1, one can convert $Sa(T^*,5\%)$ to $Sa(T_1,5\%)$ on a record-by-record basis as mentioned in Fragiadakis et al. [23]. The resulting IDA curves of the ESDOF model are presented in Fig. 3a by the continuous grey lines, while the black color indicates the 16, 50 and 84% IDA fractiles. Note the grey rectangle that highlights the zero variability in the ESDOF response at low IM values since in this region it behaves elastically.

For comparison purposes, the MDOF model is also subjected to IDA using the same set of ground motion records; the resulting IDA curves and fractiles are shown in Fig. 3b. The IDA fractiles of both MDOF and SDOF systems are presented in Fig. 3c. The 50% IDA fractiles of ESDOF and MDOF model do not coincide, thus bias is introduced in the median estimate of the ESDOF response. In fact, obtaining the exact same response from both models would be quite fortuitous since multiple approximations are involved in the ESDOF approach. For the case at hand, the use of the ESDOF leads to conservative estimates. Of course, this outcome cannot be generalized since it depends on multiple factors, such as the backbone curve used to fit the SPO curve since different piecewise approximations would lead in differences in the ESDOF's response. This discrepancy is also attributed to the load pattern employed for progressively loading the MDOF model to obtain the SPO. In our case a first-mode proportional lateral load pattern was adopted, however adaptive load patterns that would allow accounting for the stiffness degradation, the change of the modal characteristics and the period elongation of the structure [24, 25] could potentially better reproduce the behaviour of the structure in the negative stiffness segment. Regardless of the approach adopted, though, such biases are to be expected whenever an ESDOF is used in place of an MDOF. Of more interest is how one could take advantage of the MDOF to remove the bias without incurring a high computational cost.

4. Fragility assessment via mixed modelling

The 5-parameter model of Jalayer and Cornell [26] treats no-collapse and collapse data separately: a power-law approximation (3 parameters) is fit to the no-collapse data for estimating the probability of exceeding the limit state of interest given that collapse has not occurred for a given IM level. The probability of collapse is determined by fitting an ideally lognormal distribution on the collapse data, thus reducing it to its median value and dispersion (2 parameters). The mutually exclusive events of collapse, C, and no collapse, NC, are combined through Eq. (3) to obtain the probability of exceeding the LS of interest given the IM as:

$$\mathrm{P}[EDP > EDP_C \mid IM] = \mathrm{P}[EDP > EDP_C \mid NC, IM] \cdot (1 - \mathrm{P}[C \mid IM]) + 1 \cdot \mathrm{P}[C \mid IM] \quad (3)$$

where P[$EDP > EDP_c \mid C,IM$] is the probability that the EDP exceeds the EDP capacity, EDP_C, given that collapse has occurred; this always equals 1. P[$EDP > EDP_C \mid IM$] is the probability of the EDP demand exceeding EDP_C given the IM, while P[$EDP > EDP_C \mid NC,IM$] is the probability that the EDP demand exceeds the EDP_C for a certain IM level given that collapse has not occurred, and P[$C \mid IM$] is the probability of collapse given the IM.

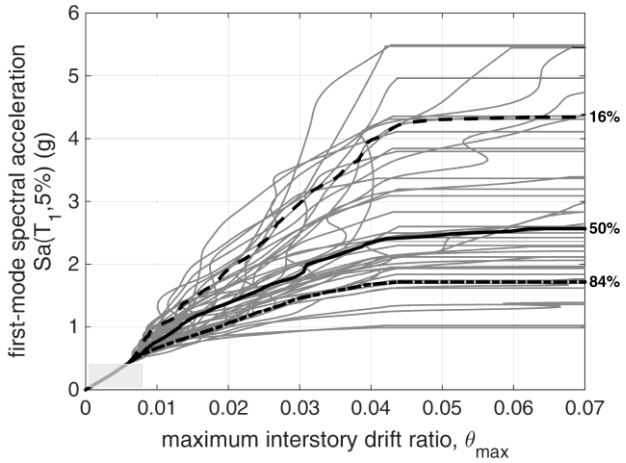

(a) IDA results of the ESDOF model

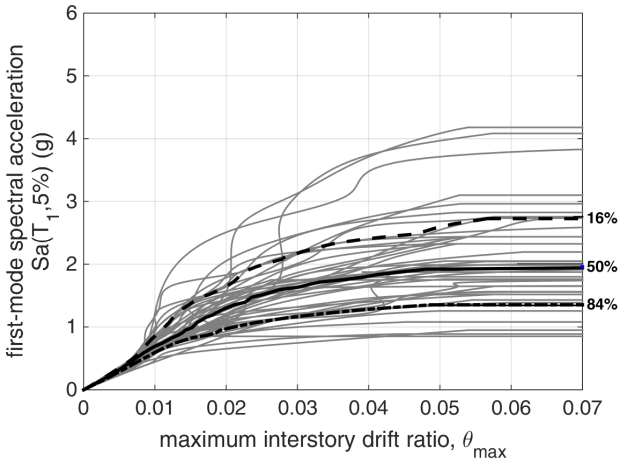

(b) IDA results of the MDOF model

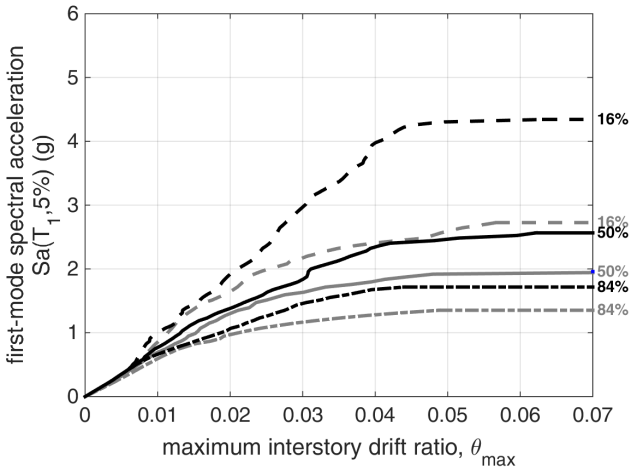

(c) comparison of the IDA fractiles of the ESDOF (grey) and MDOF (black) model

Fig. 3 – Incremental Dynamic Analysis results in terms of the first-mode spectral acceleration of the MDOF model and maximum interstory drift ratio, θ_{max}, along with the 16%, 50% and 84% IDA fractiles for both ESDOF and MDOF models

The P[$EDP > EDP_C \mid NC,IM$] term is estimated by employing a power-law fit to the no collapse data, as proposed by [27]:

$$EDP = a \cdot IM^{b}\varepsilon \tag{4}$$

where b is the slope in log-log space, ln(a) is the intercept and ε is a lognormal random variable with unit median and a logarithmic standard deviation of $\sigma_{\ln\varepsilon}$. The basic assumption of this approach is that the $EDP \mid IM$ dispersion is constant for all IM levels hence by globally applying Eq. (4) a constant dispersion is assumed over all IMs.

Global collapse is generally deemed to occur when numerical non-convergence appears in a rigorous model that incorporates both material and geometric nonlinearities or unrealistically large values of EDP are captured. Such large or infinite EDPs would bias the results at lower IMs (or even make the fitting impossible) if a single regression was to be applied to all data. To overcome this issue, the probability of collapse is estimated directly from collapse points. Multiple methods have been proposed for fitting the

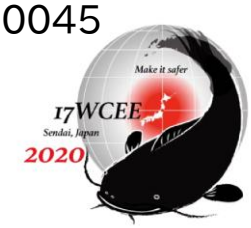

collapse data most notably the logistic regression, the maximum likelihood estimation (MLE) or the method of moments [28]. MLE is employed herein for fitting the lognormal distribution to the collapse data, whose median and the dispersion are estimated as the parameters that maximize the likelihood function [28]:

$$\left\{\hat{\theta},\hat{\beta}\right\}=\arg\max_{\theta,\beta}\sum_{j=1}^{m}\left\{\ln\binom{n_j}{z_j}+z_j\ln\Phi\left(\frac{\ln\left(x_j/\theta\right)}{\beta}\right)+\left(n_j-z_j\right)\ln\left(1-\Phi\left(\frac{\ln\left(x_j/\theta\right)}{\beta}\right)\right)\right\} \quad (5)$$

where $\hat{\theta}$ and $\hat{\beta}$ are the estimates of the mean, θ, and the standard deviation, β, of the logarithmic fragility distribution of the collapse data, $\varphi(\ )$ and $\Phi(\ )$ denote the probability density function and the cumulative density function of the standard normal distribution, respectively, n_j are the number of ground motions per $IM = x_j$, z_j is the number of ground motions that caused structural collapse for $IM = x_j$ and m is the number of IM levels. This fit can be realized, e.g., in MATLAB® via the generalized linear regression with a probit link. The probit link is used for fitting the normal distribution, or equivalently the lognormal distribution if the natural logarithm of the data is the input.

The analysis results of the ESDOF model are of low fidelity, thus even a single stripe of dynamic analyses can be performed on the MDOF system to obtain higher fidelity information on the structural response. Given the computational restrictions, a limited number of dynamic analyses, say e.g. 7, can be performed and used for refining the response obtained by the ESDOF. Such few analyses can still provide a fairly accurate estimate of the median EDP | IM distribution; yet they are not adequate to assess the dispersion, which is generally underestimated by small samples. There are cases where even a small sample may offer a viable estimate of dispersion, especially when stratified sampling has been employed as a by-product of ground motion record selection. The Conditional Spectrum approach of Lin et al. [4] is such an example due to the process involved in selecting the records. Nevertheless, for reasons of generality, we shall only employ the MDOF model outputs for updating the median estimate of ESDOF, but not for improving the estimate of the variability. To this effect, we selectively assimilate the MDOF stripe results into the 5-parameter model whose variables as shown in Table 1.

Table 1 – How each parameter of the five-parameter model is determined

Parameter	Data/Fit	MDOF or ESDOF model?
a	Non-collapse data power-law regression fit	MDOF
b		ESDOF
$\sigma_{\ln\varepsilon}$		ESDOF
θ	Collapse data MLE fit	if collapse data available MDOF, else ESDOF
β		ESDOF

Specifically, regarding the distribution of no collapse given IM, by fitting the power-law based approximation to the no-collapse points of the ESDOF model, the parameters b_{ESDOF}, a_{ESDOF} and $\sigma_{\ln\varepsilon\text{-}ESDOF}$ are estimated. When taking into account the stripe analysis of the MDOF model we can substitute a_{ESDOF} by the a_{MDOF} value obtained through the MDOF stripe, while maintaining the other two parameters. Consequently, the mixed power-law-based approximation is described by b_{ESDOF}, a_{MDOF} and $\sigma_{\ln\varepsilon\text{-}ESDOF}$. This way, we account for the median estimate of the MDOF's response while not changing the variability. When it comes to collapse data, if none of the records has caused structural collapse on the MDOF model, the distribution of collapse given IM is directly obtained through the MLE fit of the ESDOF. One could potentially still redo

the MLE fit while incorporating the absence of collapse at the stripe's IM level, yet this is usually too much trouble for little added benefit. On the other hand, if collapse has been observed on the MDOF stripe, the probability of collapse can be estimated as:

$$\mathrm{P}_{stripe}[C \mid IM_{stripe}] = \frac{N_{EDP>EDPcollapse}}{N_{total}} \tag{6}$$

where $N_{EDP>EDPcollapse}$ are the number of collapse points, N_{total} are the total number of points in the stripe and IM_{stripe} is the IM level of the stripe. This P_{stripe}-IM_{stripe} point estimate can be used for updating the distribution of collapse obtained from the ESDOF model, simply by changing its median value in order for the corresponding fragility to pass through the point estimate while maintaining the dispersion constant. This option is schematically shown in Fig. 4. Obviously, the further away this point estimate is from the median (i.e. a P_{stripe} = 0.5), the more haphazard such an approach becomes, as a tail-point would be used to bias correct a central value.

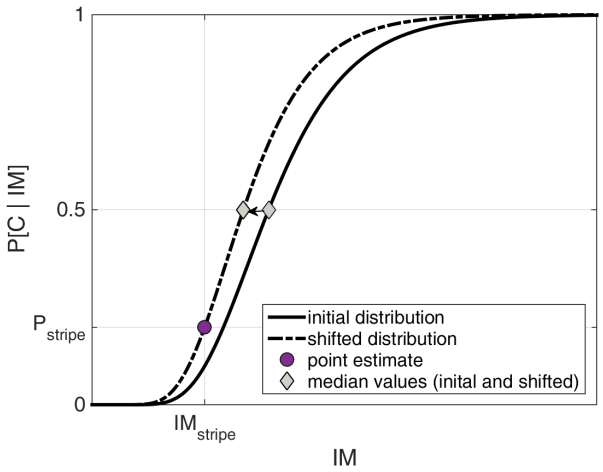

Fig. 4 – Schematic representation of updating the probability of collapse to match the point estimate. The median of the lognormal fragility curve (grey diamond point) is shifted to match the point estimate (purple bullet point) while the dispersion is maintained constant

5. Application on the 4-story building

A stripe analysis is performed on the MDOF model at the IM level with 10% probability of exceedance in 50 years, as estimated from the site-specific seismic hazard curve. Seven records are randomly selected from the far-field ground motion set of FEMA P695 [22] each coming from a different earthquake, and applied on the MDOF model after being scaled to the IM level of interest, to obtain the EDP | IM response. Horizontal stripes of EDP | IM are also generated from the ESDOF model's IDA results for IM values linearly spaced within 0.1 and 6.0g with a step of 0.1g. The stripe analysis results of the MDOF model are presented in Fig. 5a by the magenta triangle points, while the ESDOF stripes are shown in grey. Note that the light grey is used for the stripes with more than 16% of collapses while the dark grey for the others. The power law approximation is fit to the no-collapse stripes of the ESDOF model having less than 16% of collapses and the 3 parameters b_{ESDOF}, a_{ESDOF} and $\sigma_{\ln\varepsilon\text{-}ESDOF}$ are estimated. The single stripe on the MDOF model is of higher fidelity and it is used for updating the estimate of a_{ESDOF} to a_{MDOF}. Regarding collapse data, since none of the records caused structural collapse on the MDOF, the probability of collapse is directly obtained from the ESDOF model.

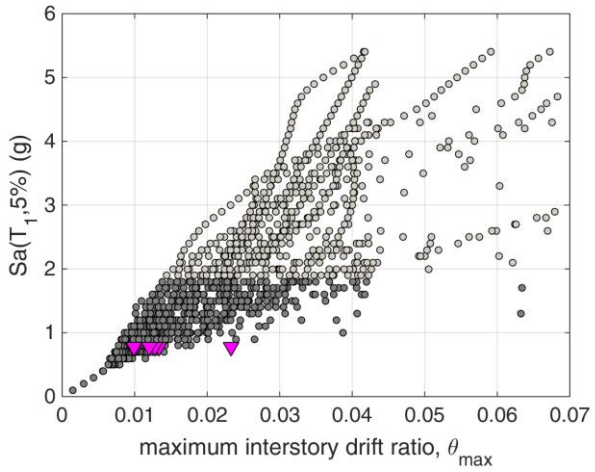

(a) Stripe analysis results of ESDOF (light/dark grey for stripes with more/less than 16% collapses) and the MDOF model (magenta)

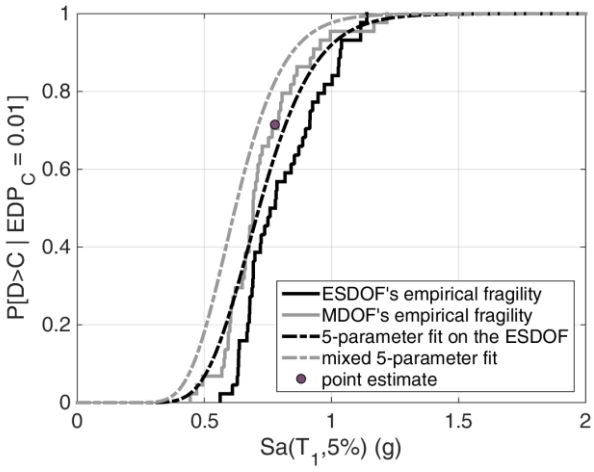

(b) fragility curves for EDP_C = 1.0%

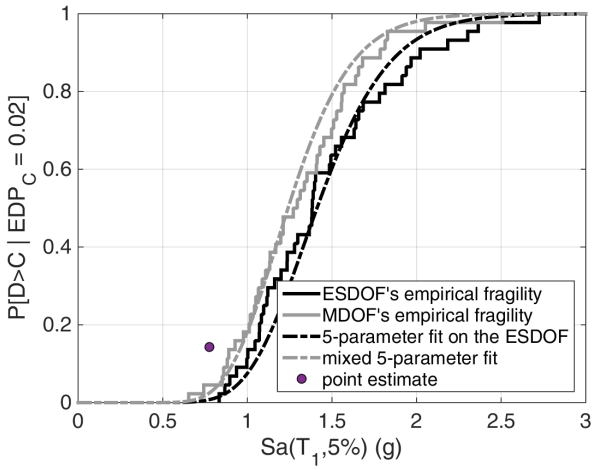

(c) fragility curves for EDP_C = 2.0%

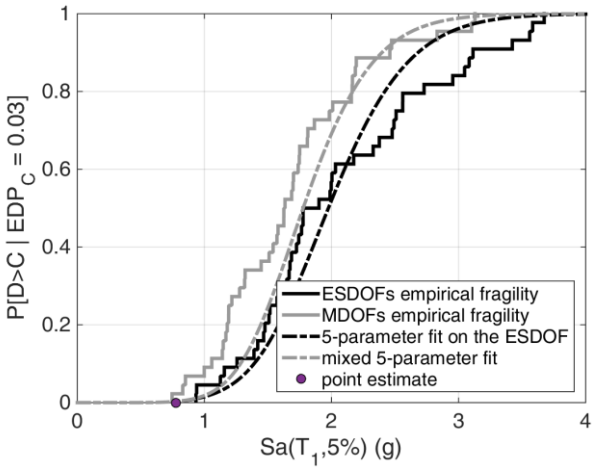

(d) fragility curves for EDP_C = 3.0%

Fig. 5 – Stripe analysis results of the ESDOF and the MDOF model and fragility curves for limit states with EDP_C equal to 1.0, 2.0 and 3.0%

Four limit states are examined to illustrate the proposed framework, covering a wide range of structural response, namely EDP_C = 0.01, 0.02 and 0.03. In Fig. 5b-d the resulting fragility curves are presented. In each of these figures, the continuous black line is used for plotting the empirical fragility curve obtained from a vertical stripe for the given EDP_C through the ESDOF IDA results, the continuous grey line for the empirical fragility of MDOF IDA results (when subjected to the 44 records), the dash-dotted black line shows the results of the 5-parameter fit on the ESDOF model and dash-dotted grey line is used for plotting the fragility curves obtained from the mixed 5-parameter fit. A point estimate of the LS fragility via the MDOF stripe results is also presented in Fig. 5b-d.

It can be observed that for the case at hand, the fragility estimates of the ESDOF model are conservative relative to the ones of the MDOF model. For all limit states the empirical fragility of the ESDOF is shifted to the right side, when compared to MDOF's. The dispersion estimate of the ESDOF model is close to the one of the MDOF model, since the slopes of the empirical fragilities are more or less close to each other. The 5-parameter approximation of the ESDOF model captures the empirical fragilities well enough for all limit states, despite the simplifications it involves: We only use 5-parameters to fit a more

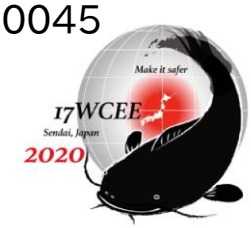

complicated distribution. Overall, the mixed power-law based approximation results in fragilities that are shifted to the left (i.e., they are more aggressive) in comparison to those of the ESDOF model, offering an improved estimate on the response of the structure closer to the one obtained from pure MDOF IDA results. Of course, inherent limitations lie within this concept since shooting for EDP_C values outside the EDP range of the stripe of which not enough data is available, may lead to errors in the estimate. Finally, the point estimates in the same figures indicate that the distribution of the EDP | IM cannot be considered reliable when a limited number of analyses are run on the stripe, thus shifting the lognormal fragility curves based on this point estimates should not be considered unless considerably more records are employed. In such cases, though, it would become a question whether one should employ much information from the ESDOF results, as well as whether one could easily divide such rich stripes into two or more sparser ones to get a wider estimate that would ultimately render the ESDOF approximation mute.

6. Conclusions

The presented approach can be used for combining different analysis options into a single output suitable for fragility assessment. In this case, the example shown by the five-parameter power-law-based model enabled obtaining reliable estimates of the fragility curves while using the equivalent SDOF model results as a basis to be updated by a single sparse stripe analysis on the MDOF model. The value of this approach becomes more apparent when considering highly complex models where each response history analysis comes at a considerable cost, and taking advantage of every single point estimate available is of paramount importance.

7. Acknowledgements

Financial support has been provided by the Innovation and Networks Executive Agency (INEA) under the powers delegated by the European Commission through the Horizon 2020 program “PANOPTIS–Development of a decision support system for increasing the resilience of transportation infrastructure based on combined use of terrestrial and airborne sensors and advanced modelling tools”, Grant Agreement number 769129. The second author also acknowledges the financial support provided by the Eugenides Foundation in Greece.

8. References

[1] Cornell CA, Krawinkler H (2000): Progress and Challenges in Seismic Performance Assessment. *PEER Center News 2000*, **3** (2), 1-4.

[2] Bakalis K, Vamvatsikos D (2018): Seismic fragility functions via nonlinear dynamic methods. *ASCE Journal of Structural Engineering*, **144** (10), 04018181. DOI: 10.1061/(ASCE)ST.1943-541X.0002141

[3] Baker JW, Cornell CA (2006): Spectral shape, epsilon and record selection. *Earthquake Engineering and Structural Dynamics*, **35** (9), 1077-1095. DOI: 10.1002/eqe.571

[4] Lin T, Haselton CB, Baker JW (2013): Conditional spectrum-based ground motion selection. Part I: Hazard consistency for risk-based assessments. *Earthquake Engineering and Structural Dynamics*, **42** (12), 1847-1865. DOI: 10.1002/eqe.2301

[5] Kohrangi M, Bazzurro P, Vamvatsikos D, Spillatura A (2017): Conditional spectrum-based ground motion record selection using average spectral acceleration. *Earthquake Engineering and Structural Dynamics*, **46** (10), 1667-1685. DOI: 10.1002/eqe.2876

[6] Krawinkler H, Seneviratna GDPK (1998): Pros and cons of a pushover analysis of seismic performance evaluation. *Engineering Structures*, **20** (4-6), 452-464. DOI: 10.1016/S0141-0296(97)00092-8

[7] Fragiadakis M, Vamvatsikos D, Ascheim M (2014): Application of nonlinear static procedures for the seismic assessment of regular RC moment frame buildings. *Earthquake Spectra*, **30** (2), 767-794. DOI: 10.1193/111511EQS281M

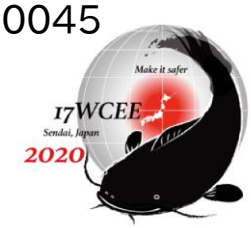

[8] ASCE 41-13 (2014): *Seismic Evaluation and Retrofit of Existing Buildings*. American Society of Civil Engineers, Reston, VA.

[9] EN1998-3 (2005): *Eurocode 8: Design of structures for earthquake resistance - Part 3: Assessment and retrofitting of buildings*. European Committee for Standardization, Brussels

[10] De Luca F, Vamvatsikos D, Iervolino I (2013): Near-optimal piecewise linear fits of static pushover capacity curves for equivalent SDOF analysis. *Earthquake Engineering and Structural Dynamics*, **42** (4): 523-543. DOI: 10.1002/eqe.2225

[11] Ruiz-García J, Miranda E (2007): Probabilistic estimation of maximum inelastic displacement demands for performance-based design. *Earthquake Engineering and Structural Dynamics*, **36** (9), 1235-1254. DOI: 10.1002/eqe.680

[12] Vamvatsikos D, Cornell CA (2006): Direct estimation of the seismic demand and capacity of oscillators with multi-linear static pushovers through IDA. *Earthquake Engineering*, **35** (9), 1097-1117. DOI: 10.1002/eqe.573

[13] Baltzopoulos G, Baraschino R, Iervolino I, Vamvatsikos D (2018): Dynamic analysis of single-degree-of-freedom systems (DYANAS): A graphical user interface for OpenSees. *Engineering Structures*, **177**, 395-408. DOI: 10.1016/j.engstruct.2018.09.078

[14] Baltzopoulos G, Baraschino R, Iervolino I, Vamvatsikos D (2017): SPO2FRAG: Software for seismic fragility assessment based on static pushover. *Bulletin of Earthquake Engineering*, **15** (10), 4399-4425. DOI: 10.1007/s10518-017-0145-3

[15] Aschheim M, Hernández-Montes E, Vamvatsikos D (2019): *Design of Reinforced Concrete Buildings for Seismic performance: Practical, deterministic and probabilistic approaches*, CRC Press.

[16] Vamvatsikos D, Aschheim M (2016): Performance-based seismic design via yield frequency spectra. *Earthquake Engineering and Structural Dynamics*, **45** (11), 1759-1778. DOI: 10.1002/eqe.2727

[17] Mazzoni S, McKenna F, Scott M, Fenves G (2000): *Open system for earthquake engineering simulation: OpenSees command language manual*, University of California, Berkeley, CA.

[18] Fajfar P (2000): A nonlinear analysis method for performance-based seismic design. *Earthquake Spectra*, **16** (3), 573-592. DOI: 10.1193/1.1586128

[19] Vamvatsikos D, Cornell CA (2002): Incremental dynamic analysis. *Earthquake Engineering & Structural Dynamics*, **31** (3), 491-514. DOI: 10.1002/eqe.141

[20] Vamvatsikos D (2011): IDA Matlab running routines for OpenSEES. Available at: http://users.ntua.gr/divamva/software/bundle_runIDA.zip

[21] Vamvatsikos D, Cornell CA (2004): Applied Incremental Dynamic Analysis. *Earthquake Spectra*, **20** (2), 523-553. DOI: 10.1193/1.1737737

[22] FEMA (2009). FEMA P695 Far field ground motion set. Available at: http://users.ntua.gr/divamva/resourcesRCbook/FEMA-P695-FFset.zip

[23] Fragiadakis M, Vamvatsikos D, Papadrakakis M (2006): Evaluation of the influence of vertical irregularities on the seismic performance of a 9-storey steel frame. *Earthquake Engineering and Structural Dynamics*, **35** (12), 1489-1509. DOI: 10.1002/eqe.591

[24] Elnashai AS (2001): Advanced inelastic static (pushover) analysis for earthquake applications. *Structural Engineering and Mechanics*, **12** (1), 51-69. DOI: 10.12989/sem.2001.12.1.051

[25] Vamvatsikos D, Cornell CA (2005): Direct estimation of seismic demand and capacity of multidegree-of-freedom systems through incremental dynamic analysis of single degree of freedom approximation. *Journal of Structural Engineering*, **131** (4), 589-599. DOI: 10.1061/(ASCE)0733-9445(2005)131:4(589)

[26] Jalayer F, Cornell CA (2009): Alternative non-linear demand estimation methods for probability-based seismic assessments. *Earthquake Engineering and Structural Dynamics*, **38** (8), 951-972. DOI: 10.1002/eqe.876

[27] Cornell CA, Jalayer F, Hamburger RO, Foutch DA (2002): Probabilistic basis for 2000 SAC Federal Emergency Management Agency steel moment frame guidelines. *ASCE Journal of Structural Engineering*, **128** (4), 526-533. DOI: 10.1061/(ASCE)0733-9445(2002)128:4(526)

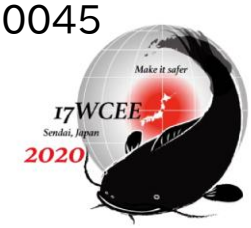

[28] Baker JW (2015): Efficient analytical fragility function fitting using dynamic structural analysis. *Earthquake Spectra*, **31** (1), 579-599. DOI: 10.1193/021113EQS025M

